Tellus (1992), *44A*, 314–323

Local error growth in a barotropic model

By JAN BARKMEIJER, *Royal Netherlands Meteorological Institute, PO Box 201, 3730 AE De Bilt, The Netherlands*

(Manuscript received 18 April 1991; in final form 16 December 1991)

ABSTRACT

The concept of local error growth is considered within the context of the non-viscous barotropic vorticity equation. Using the adjoint equation of the tangent linear barotropic vorticity equation, we determine error patterns in the initial state that result in the maximum linear error growth at some pre-chosen geographical area and prediction time. For some solutions of the nonlinear barotropic vorticity equation, we investigate to what extent error growth depends on the geographical position of the area considered. It appears that for short prediction times (<3 days), the barotropic growth of kinetic energy of initial perturbations is exponential plus a substantial transient effect due to the non-orthogonality of the eigenmodes of the tangent linear operator with respect to the kinetic energy inner product. The latter mechanism initially causes very rapid perturbation growth, even for neutral flows.

1. Introduction

Weather forecasting is subject to several mechanisms which degrade the quality of the forecast after some time. On average, the doubling time for small root-mean-square errors in the temperature and wind fields is of the order of two days. Error growth is partly caused by the imperfection of the forecast model. Improving the model description or careful handling of the data output may reduce this error somewhat (Thiébaux and Morone, 1990). Another major reason of error growth is the instability of the flow, its sensitive dependence on initial conditions. Starting from almost identical initial conditions, flow fields may diverge from each other so that after integrating only a few days, little resemblance between the various final states remains. The impact of this intrinsic error growth on weather forecasting was first pointed out by Lorenz (1963).

In what follows, we shall concentrate on the intrinsic errors of the model. For this study, we limit ourselves to linear error growth. Lacarra and Talagrand (1988) make the assumption of linear error growth plausible for ranges up to two days. For a review of methods in the non-linear regime, we refer to Palmer and Tibaldi (1988).

The study of error growth requires a choice for its measure. One way to analyse the robustness of solutions of forecast models, is to consider the time evolution of the kinetic energy of initial errors. Evidently, this measure of error growth is global in nature. With local measures it is possible to study regional variations in error growth due to variations in local stability. It is then possible to focus on forecast quality in certain geographical locations.

In this paper we introduce the notion of *local error growth*. By this we mean error growth in a restricted geographical area; the final error field outside this area is of no concern. For simplicity we restrict this study to local error growth in a barotropic model. It turns out to be useful to employ the so-called adjoint equations. These equations provide an efficient tool in determining the gradient of a multi-variable function. During the past years the adjoint equations have been utilized in studying various problems such as the sensitivity of atmospheric models to variations in the physical parameters (Hall and Cacuci, 1983), or data assimilation (Talagrand and Courtier, 1987; Le Dimet and Talagrand, 1986).

Before we apply this technique to the barotropic vorticity equation in Section 3, we explain it in a more general setting in Section 2. In Section 4, the concept of local error growth is introduced and in Section 5 we present some numerical results. Finally, some concluding remarks are presented in Section 6.

2. The adjoint equation

Suppose the dynamics of a model is described in such a way that the evolution equation can be represented as:

$$\frac{dx}{dt} = F(x). \tag{1}$$

Here, $F: \mathscr{H} \mapsto \mathscr{H}$ is a differentiable function defined on a Hilbert space $\mathscr{H}$. The inner product of $\mathscr{H}$ we denote by $\langle\, , \rangle$. The adjoint equation depends on the choice of this inner product, see the appendix.

Let $x(t)$ be a solution of eq. (1). In case we add a small perturbation $\varepsilon(0)$ to $x(0)$, the time evolution of $\varepsilon(t)$ to first order with respect to $\varepsilon(0)$ is given by the so-called tangent linear equation:

$$\frac{d\varepsilon}{dt} = F'(t)\,\varepsilon. \tag{2}$$

The linear operator $F'(t)$ is obtained by differentiating F along the solution $x(t)$ of eq. (1). Since eq. (2) is linear, we may write

$$\varepsilon(t_2) = R(t_1, t_2)\,\varepsilon(t_1), \qquad 0 \leqslant t_1 \leqslant t_2 \leqslant t,$$

where $R(t_1, t_2)$ is a linear operator. The operator R is called the resolvent of eq. (2).

Given a linear operator $L: \mathscr{H} \to \mathscr{H}$, we define a linear operator $L^*: \mathscr{H} \to \mathscr{H}$ by:

$$\langle Lx, y\rangle = \langle x, L^*y\rangle \qquad \text{for all} \quad x, y \in \mathscr{H}.$$

The operator L^* is uniquely determined and is called the adjoint of L. Observe that L^* depends on the inner product of $\mathscr{H}$. If $L^* = L$ the operator is called self-adjoint. Further it is a direct consequence of the definition that $(AB)^* = B^*A^*$.

The *adjoint equation* of eq. (2) is now given by:

$$\frac{d\tilde{\varepsilon}}{dt} = -F'^*(t)\,\tilde{\varepsilon}. \tag{3}$$

For any two solutions ε and $\tilde{\varepsilon}$ of eq. (2) and the adjoint equation eq. (3) respectively, we have

$$\frac{d}{dt}\langle \varepsilon(t), \tilde{\varepsilon}(t)\rangle = \langle F'(t)\,\varepsilon(t), \tilde{\varepsilon}(t)\rangle + \langle \varepsilon(t), -F'^*(t)\,\tilde{\varepsilon}(t)\rangle = 0.$$

As in the case of eq. (2), we can define the resolvent of eq. (3) which we denote by S. The solution of eq. (2) with initial condition x at time t_1 equals $R(t_1, t_2)x$ at time t_2. Whereas the solution of eq. (3) with initial condition y at time t_2 equals $S(t_2, t_1)y$ at time t_1. Since the inner product between solutions of eqs. (2) and (3) remains constant in time, we may write:

$$\langle R(t_1, t_2)\,x, y\rangle = \langle x, S(t_2, t_1)\,y\rangle \quad \text{for all} \quad x, y \in \mathscr{H}.$$

Consequently $S(t_2, t_1)$ is the adjoint of $R(t_1, t_2)$. So in order to determine $R^*(t_1, t_2)\,\varepsilon$ it suffices to integrate the adjoint equation (3) backwards in time from time t_2 to time t_1 and with final condition ε.

3. The adjoint equation of the barotropic vorticity equation

The barotropic vorticity equation,

$$\frac{\partial \zeta}{\partial t} = \mathscr{J}(\zeta + f, \Delta^{-1}\zeta), \tag{4}$$

describes the dynamics of a two-dimensional non-divergent and inviscid flow at the surface of a rotating sphere S^2. In eq. (4), ζ is the relative vorticity and f is the Coriolis parameter. The Jacobi operator $\mathscr{J}$ is defined by

$$\mathscr{J}(g, h) = \frac{\partial g}{\partial \lambda}\frac{\partial h}{\partial \mu} - \frac{\partial g}{\partial \mu}\frac{\partial h}{\partial \lambda},$$

where λ is the geographic longitude and μ is the sine of the geographic latitude. We use the radius of the earth as unit of length and the inverse of the angular speed of rotation of the earth as unit of time. The relative vorticity ζ is related to a streamfunction ψ through $\Delta\psi = \zeta$. In the sequel we do all computations in terms of streamfunctions.

Suppose $\psi(t)$ is a solution of eq. (4). Linearizing around $\psi(t)$ we obtain the tangent linear equation:

$$\frac{\partial \varepsilon}{\partial t} = \Delta^{-1}\mathscr{J}(\Delta\varepsilon, \psi) + \Delta^{-1}\mathscr{J}(\Delta\psi + f, \varepsilon). \tag{5}$$

In order to define the adjoint equation we have to select an inner product for functions on S^2. For convenience we work with functions that are at least twice differentiable. Possible choices for such an inner product are

$$\langle f, g\rangle_n = \frac{1}{4\pi}\iint_{S^2} \nabla^n f \cdot \nabla^n g \, \mathrm{d}s, \qquad n = 0, 1, 2.$$

The subscript $n = 0$ corresponds to the squared norm, $n = 1$ to the kinetic energy norm and $n = 2$ to the enstrophy norm. Unless stated otherwise we will use the kinetic energy inner product and denote it by $\langle\ ,\ \rangle$. The Laplacian operator Δ is self-adjoint with respect to this inner product:

$$\langle \Delta f, g\rangle = \frac{1}{4\pi}\iint_{S^2} \nabla(\Delta f) \cdot \nabla g \, \mathrm{d}s$$

$$= -\frac{1}{4\pi}\iint_{S^2} \Delta f \cdot \Delta g \, \mathrm{d}s$$

$$= \frac{1}{4\pi}\iint_{S^2} \nabla f \cdot \nabla(\Delta g) \, \mathrm{d}s = \langle f, \Delta g\rangle.$$

Further the Jacobi operator has the property that for all functions f, g and h that are at least twice differentiable:

$$\iint_{S^2} \mathscr{J}(f, g)\, h \, \mathrm{d}s = \iint_{S^2} f \mathscr{J}(g, h) \, \mathrm{d}s. \tag{6}$$

This follows from the following identities:

$$\iint_{S^2} \mathscr{J}(f, g)\, h \, \mathrm{d}s = \iint_{S^2} \left[\frac{\partial f}{\partial \lambda}\frac{\partial g}{\partial \mu} - \frac{\partial f}{\partial \mu}\frac{\partial g}{\partial \lambda}\right] h \, \mathrm{d}s$$

$$= -\iint_{S^2} f \frac{\partial^2 g}{\partial \lambda\, \partial \mu} h \, \mathrm{d}s - \iint_{S^2} f \frac{\partial g}{\partial \mu}\frac{\partial h}{\partial \lambda} \, \mathrm{d}s$$

$$+ \iint_{S^2} f \frac{\partial^2 g}{\partial \lambda\, \partial \mu} h \, \mathrm{d}s + \iint_{S^2} f \frac{\partial g}{\partial \lambda}\frac{\partial h}{\partial \mu} \, \mathrm{d}s$$

$$= \iint_{S^2} f \left[\frac{\partial g}{\partial \lambda}\frac{\partial h}{\partial \mu} - \frac{\partial g}{\partial \mu}\frac{\partial h}{\partial \lambda}\right] \mathrm{d}s$$

$$= \iint_{S^2} f \mathscr{J}(g, h) \, \mathrm{d}s.$$

In deriving the adjoint equation of eq. (4), it suffices to determine the adjoint of the linear operator $\varepsilon \to \mathscr{J}(\varepsilon, \psi)$. With eq. (6), we can write:

$$\langle \mathscr{J}(\varepsilon, \psi), \varepsilon'\rangle = \frac{1}{4\pi}\iint_{S^2} \nabla \mathscr{J}(\varepsilon, \psi) \cdot \nabla \varepsilon' \, \mathrm{d}s$$

$$= -\frac{1}{4\pi}\iint_{S^2} \mathscr{J}(\varepsilon, \psi)\, \Delta\varepsilon' \, \mathrm{d}s$$

$$= -\frac{1}{4\pi}\iint_{S^2} \varepsilon\, \Delta(\Delta^{-1}\mathscr{J}(\psi, \Delta\varepsilon')) \, \mathrm{d}s$$

$$= \frac{1}{4\pi}\iint_{S^2} \nabla\varepsilon \cdot \nabla(\Delta^{-1}\mathscr{J}(\psi, \Delta\varepsilon')) \, \mathrm{d}s$$

$$= \langle \varepsilon, \Delta^{-1}\mathscr{J}(\psi, \Delta\varepsilon')\rangle.$$

So the adjoint of $\varepsilon \mapsto \mathscr{J}(\varepsilon, \psi)$ is equal to the operator $\varepsilon' \mapsto \Delta^{-1}\mathscr{J}(\psi, \Delta\varepsilon')$. Using $(LM)^* = M^*L^*$ and the fact that Δ is self-adjoint, we conclude that the adjoint of eq. (4) reads as:

$$\frac{\partial \varepsilon'}{\partial t} = \mathscr{J}(\varepsilon', \psi) + \Delta^{-1}\mathscr{J}(\Delta\psi + f, \varepsilon'). \tag{7}$$

4. Local error growth

Suppose that for a time interval $[0, t]$ the error $\varepsilon(s)$, $s \in [0, t]$, of a solution of eq. (4) is known. The time evolution of the kinetic energy of $\varepsilon(s)$ is a global measure of the error growth. Increase of the error kinetic energy does not necessarily mean that errors grow uniformly over the globe. Local variations in error growth may be quite substantial. In this section we study how errors grow in a single grid position. Using the adjoint equation, we determine the initial erorr $\varepsilon(0)$ for which $\varepsilon(t)$ evaluated at a certain geographical position p (in notation $\varepsilon(t)_{|p}$) is maximized. Notice that we have to impose a constraint upon $\varepsilon(0)$. We assume that the kinetic energy of $\varepsilon(0)$ has a fixed value. The maximum error in p is probably a useful indicator of the temporal sensitivity of the forecast for the area around p. Given a constraint for the initial error it yields an upper bound for the error growth. So it can serve as a measure of local and temporal predictability of the atmospheric circulation. In addition we get information on the areas in the initial state where analysis errors substantially contribute to the forest error in p.

In the following we assume that functions on the sphere are expanded in spherical harmonics Y_{mn}, which are of the form

$$Y_{mn}(\lambda, \mu) = P_{mn}(\mu)\exp(im\lambda), \qquad m \in \mathbb{Z}$$
$$\text{and} \qquad n \geq |m|, \qquad n \in \mathbb{N}. \tag{8}$$

Here the functions P_{mn} denote the associated Legendre functions of the first kind and of order m and degree n:

$$P_{mn}(\mu) = \left[(2n+1)\frac{(n-m)!}{(n+m)!}\right]^{1/2} \times \frac{(1-\mu^2)^{m/2}}{2^n n!}\frac{\mathrm{d}^{n+m}}{\mathrm{d}\mu^{n+m}}(\mu^2-1)^n,$$

(see Machenhauer, 1979).

With respect to the inner product defined by

$$(f, g) = \frac{1}{4\pi}\iint_{S^2} f\bar{g}\,\mathrm{d}s,$$

the functions Y_{mn} form a complete orthogonal set for C^2 functions on the sphere, (Courant and Hilbert, 1953). Let $\mathscr{F}$ be the set of real-valued functions with zero mean expanded in spherical harmonics using triangular truncation of order N. Because of the zero mean we may assume in the following that the $m = n = 0$ term is omitted from all expansions $g = \sum_{m=-N}^{N}\sum_{n=|m|}^{N} g_{mn}Y_{mn}$ for $g \in \mathscr{F}$. The function $\delta \in \mathscr{F}$ which is an approximation of the Dirac function in some grid point p, is given by

$$\delta = \sum_{m=-N}^{N}\sum_{n=|m|}^{N} \bar{Y}_{mn}(p)\,Y_{mn}. \tag{9}$$

With δ, we define a linear operator $L: \mathscr{F} \mapsto \mathscr{F}$ by

$$L\varepsilon = \varepsilon_{|p} \cdot \delta. \tag{10}$$

In determining the initial error field $\varepsilon(0)$ which, after time t, results in the largest absolute grid point value in p, we make use of this operator L. The adjoint of L, which we need later on, is given by:

$$L^*\varepsilon = (\Delta\varepsilon)_{|p} \cdot \Delta^{-1}\delta. \tag{11}$$

Before we check that this indeed is the adjoint of L, we first give an expression for the inner product $\langle f, g\rangle$, with $f, g \in \mathscr{F}$, in terms of harmonic coefficients. Notice that Y_{mn} is an eigenvector of the Laplacian operator Δ with eigenvalue $a_n = -n(n+1)$ and thus:

$$\begin{aligned}\langle f, g\rangle &= \langle f, \bar{g}\rangle \\ &= \frac{-1}{4\pi}\iint_{S^2}\sum_{m=-N}^{N}\sum_{n=|m|}^{N} a_n f_{mn}Y_{mn} \\ &\quad \times \left(\sum_{k=-N}^{N}\sum_{l=|k|}^{N} \bar{g}_{kl}\bar{Y}_{kl}\right)\mathrm{d}s \\ &= -\sum_{m=-N}^{N}\sum_{n=|m|}^{N} a_n f_{mn}\bar{g}_{mn}.\end{aligned}$$

Using this expression for the inner product it is easy to see that L^*, as given by eq. (11), is the adjoint of L. For this we have to show that $\langle f, L^*g\rangle$ is equal to $\langle Lf, g\rangle$ for all $f, g \in \mathscr{F}$. This is the case:

$$\begin{aligned}\langle f, L^*g\rangle &= \langle f, \overline{L^*g}\rangle \\ &= -\sum_{m=-N}^{N}\sum_{n=|m|}^{N} a_n f_{mn} \\ &\quad \times \left[\sum_{k=-N}^{N}\sum_{l=|k|}^{N} a_l\bar{g}_{kl}\bar{Y}_{kl}(p)\right]\frac{1}{a_n}Y_{mn}(p) \\ &= -\left[\sum_{k=-N}^{N}\sum_{l=|k|}^{N} a_l\bar{g}_{kl}\bar{Y}_{kl}(p)\right]f(p) \\ &= -\sum_{k=-N}^{N}\sum_{l=|k|}^{N} a_l f(p)\,\bar{Y}_{kl}(p)\,\bar{g}_{kl} = \langle Lf, g\rangle.\end{aligned}$$

We are now able to determine the initial error $\varepsilon(0)$ that results in the largest possible error in p. Using eq. (10), we can write:

$$\begin{aligned}&\langle L\varepsilon(t), -\Delta^{-1}\varepsilon(t)\rangle \\ &= \sum_{m=-N}^{N}\sum_{n=|m|}^{N} a_n\varepsilon(t)_{|p}\bar{Y}_{mn}(p)\frac{1}{a_n}\bar{\varepsilon}_{mn}(t) \\ &= \varepsilon(t)_{|p}\sum_{m=-N}^{N}\sum_{n=|m|}^{N} \bar{\varepsilon}_{mn}(t)\,\bar{Y}_{mn}(p) \\ &= (\varepsilon(t)_{|p})^2.\end{aligned}$$

We conclude that maximizing $\langle L\varepsilon(t), -\Delta^{-1}\varepsilon(t)\rangle$ yields an initial error field that maximizes $|\varepsilon(t)_{|p}|$.

Recall that $\varepsilon(t) = R(0, t)\, \varepsilon(0)$. For convenience, we write $R = R(0, t)$. We have

$$\langle L\varepsilon(t), -\Delta^{-1}\varepsilon(t)\rangle = \langle LR\varepsilon(0), -\Delta^{-1}R\varepsilon(0)\rangle$$
$$= \langle -R^* \Delta^{-1} LR\varepsilon(0), \varepsilon(0)\rangle.$$

The operator $R^* \Delta^{-1}LR$ is self-adjoint with respect to the inner product $\langle\ ,\ \rangle$. This is a direct consequence of the following, see eq. (11):

$$R^*L^* \Delta^{-1}R\varepsilon = R^*[\Delta(\Delta^{-1}R\varepsilon)]_{|p} \cdot \Delta^{-1}\delta$$
$$= R^* \Delta^{-1}[(R\varepsilon)_{|p} \cdot \delta] = R^* \Delta^{-1}LR\varepsilon.$$

Since $R^* \Delta^{-1}LR$ is self-adjoint, the eigenvalues of $R^* \Delta^{-1}LR$ are all real. More precisely, there exists only one eigenvalue different from zero. Observe that by definition of L:

$$R^* \Delta^{-1}LR\varepsilon = (R\varepsilon)_{|p} \cdot R^* \Delta^{-1}\delta \qquad \text{for all} \quad \varepsilon \in \mathscr{F}.$$

So the operator $R^* \Delta^{-1}LR$ projects all $\varepsilon \in \mathscr{F}$ onto $R^* \Delta^{-1}\delta$. In maximizing $\langle -R^* \Delta^{-1}LR\varepsilon(0), \varepsilon(0)\rangle$ we have to look for the eigenvector of $-R^* \Delta^{-1}LR$ with largest eigenvalue. Consequently the initial error field $\varepsilon(0)$ in the direction of $R^* \Delta^{-1}\delta$ yields, when integrated to time t, the largest possible error in p.

The above can be generalized to larger areas in a straightforward manner. Let V consist of K grid points p_i, $i = 1, \dots, K$. Define a linear operator $\mathscr{L}: \mathscr{F} \mapsto \mathscr{F}$ by $\mathscr{L} = \sum_{i=1}^{K} L_i$, where

$$L_i\varepsilon = \varepsilon_{|p_i} \cdot \delta_i$$

and

$$\delta_i = \sum_{m=-N}^{N} \sum_{n=|m|}^{N} \bar{Y}_{mn}(p_i)\, Y_{mn}, \qquad i = 1, \dots, K.$$

As in the case of one grid point we can write

$$\langle \mathscr{L}\varepsilon(t), -\Delta^{-1}\varepsilon(t)\rangle = \sum_{i=1}^{K} \langle L_i\varepsilon(t), -\Delta^{-1}\varepsilon(t)\rangle$$
$$= \sum_{i=1}^{K} (\varepsilon(t)_{|p_i})^2.$$

The operator $R^* \Delta^{-1}\mathscr{L}R$ is self-adjoint and may have several eigenvalues different from zero. In fact $R^* \Delta^{-1}\mathscr{L}R$ projects onto a K-dimensional subspace of $\mathscr{F}$. The eigenvector $\varepsilon(0)$ with the largest absolute eigenvalue results, after time t, in the largest possible root-mean-square error over V.

5. Numerical experiments

In this section, we present some numerical results on local error growth. For this purpose we analysed the sensitivity to error growth of a so-called Rossby–Haurwitz wave. For given $n \geqslant |m| \geqslant 0$, these solutions of the barotropic vorticity equation are of the form:

$$\psi_{mn}(\lambda, \mu, t) = \mathrm{Re}\{Y_{mn}(\lambda - \omega t, \mu)\} - c\mu,$$

where Y_{mn} is the spherical harmonic function of order m and degree n, as defined by eq. (8), and

$$\omega = \frac{2 + c(2 - n(n+1))}{-n(n+1)}, \qquad c \in \mathbb{R}.$$

Further $\mathrm{Re}\{z\}$ denotes the real part of the complex number z.

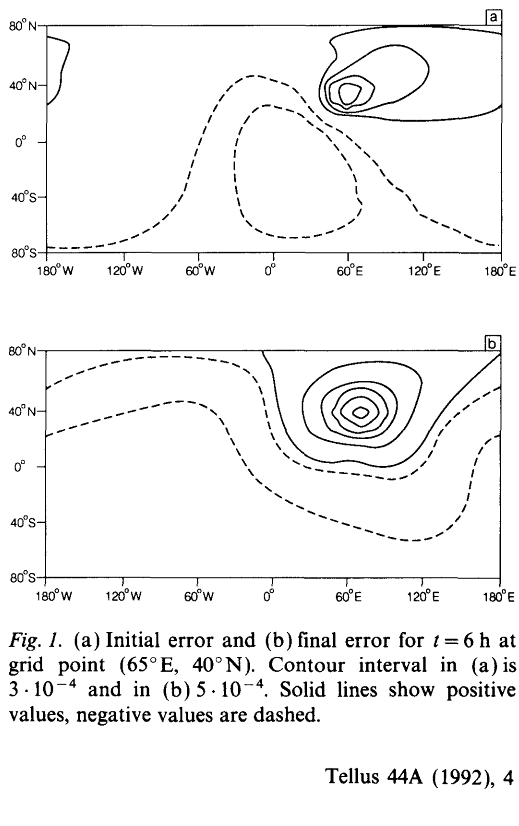

Fig. 1. (a) Initial error and (b) final error for $t = 6$ h at grid point (65°E, 40°N). Contour interval in (a) is $3 \cdot 10^{-4}$ and in (b) $5 \cdot 10^{-4}$. Solid lines show positive values, negative values are dashed.

In the following we choose $m = 2$ and $n = 3$. We also let $c = 0.2$. For these values, $\psi = \psi_{mn}$ is a stationary solution. The tangent linear equation may then we written as $(d/dt)\varepsilon = T\varepsilon$, where T is a time independent matrix and the resolvent R satisfies $R(t, s) = \exp(T(s - t))$. The amplitude of Y_{mn} is chosen in such a way that ψ is barotropically unstable. This means that the matrix T has eigenvalues with positive real part. In fact the only eigenvalues of T with positive real part are a complex pair. The corresponding growing mode has a kinetic energy e-folding time of 144 hours.

Recall that the direction of the initial error is given by $\varepsilon(0) = R^* \Delta^{-1}\delta$ and that $\varepsilon(t) = R\varepsilon(0)$. Since R is time dependent, $\varepsilon(0)$ also varies with the length of the forecast time of interest. We do our calculations of the error fields using a triangular truncation at T11. Increasing the truncation up to T21, as was used in obtaining Fig. 4, does not affect the results substantially. In all figures the initial error field was given the same kinetic energy.

Fig. 1a gives the initial error field that maximizes the forecast error at $t = 6$ h in a point p located at (65° E, 40° N), which is slightly upstream of the ridge in the stationary (2, 3)-solution, see Fig. 5. Fig. 1b displays the resulting forecast error after 6 h of integration. Observe that the initial error field is less localized than the forecast error field. The projection of the initial error pattern onto the eigenmodes of the linearized barotropic vorticity equation is such that these modes almost cancel. So components along the eigenmodes have larger

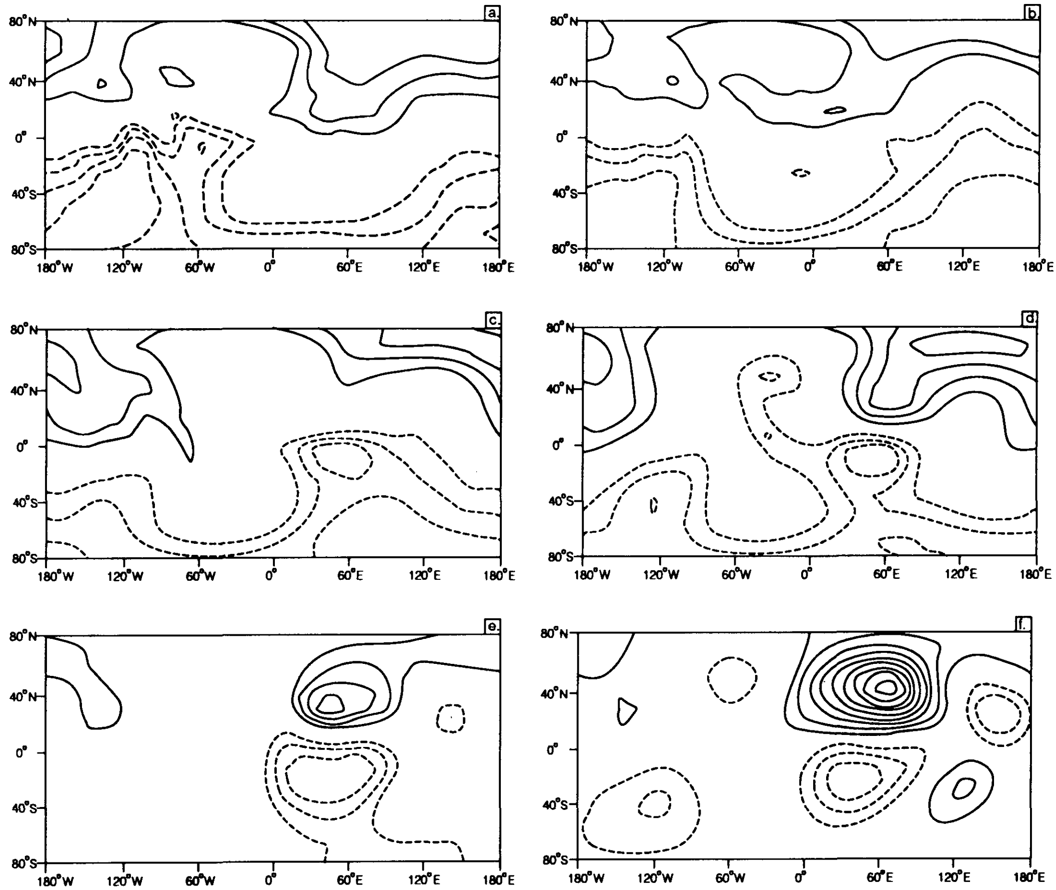

Fig. 2. Time evolution of the initial error for $t = 48$ h at grid point (65° E, 40° N). (a) 0 h, (b) 6 h, (c) 12 h, (d) 18 h, (e) 36 h and (f) 48 h. Contour interval in (a)–(d) is $3 \cdot 10^{-4}$ and in (e)–(f) $5 \cdot 10^{-4}$.

kinetic energy than the perturbation itself. This is possible because the eigenmodes are non-orthogonal with respect to the kinetic energy inner product. During the integration time they start to propagate and enhance each other maximally at the end of the integration time. This process which we call dispersion reversal, can produce very rapid error growth, (cf. Zhang, 1988; Farrell, 1990). The growth rate easily can be a factor of 10 larger than was to be expected from exponential mode growth. In experiments that we performed with a neutral flow, a similar rapid initial growth of the error field was observed. This was also found by Farrell (1987). Notice that if an inner product was chosen for which the eigenmodes are orthogonal, the error growth of a given perturbation is at the most equal to the growth of the fastest mode of the tangent linear operator.

The dispersion reversal becomes clearer for longer integration times. Fig. 2 shows the time evolution of the initial error field in $p = (65°\text{E}, 40°\text{N})$ for a forecast time of 48 h. Initially the error kinetic energy is spread over the globe but at the end of the forecast time the error has concentrated at a few relatively small areas and has grown considerably. The kinetic energy of the final error has increased by a factor 5.89. Most of the error kinetic energy is in the area around p.

Similar growth of errors occurs for other locations of p. Fig. 3a, b gives the initial and final error pattern for $p = (35°\text{W}, 40°\text{N})$, which is slightly upstream of the trough in the stationary (2, 3)-solution, see Fig. 5. The error kinetic energy is focussed in the area around p after the 48 h of integration time.

As mentioned before the amplitude of the (2, 3)-wave is chosen in such a way that the wave is unstable. All eigenvalues of T, the tangent linear operator, apart from one complex conjugated pair, have zero real parts. So there is one unique growing mode. For $t \to \infty$, the forecast error must be dominated by this exponentially growing mode. Fig. 4a shows the initial error field for p at $(65°\text{E}, 40°\text{N})$ and a forecast time of 600 h. In Fig. 4b the increase of the kinetic energy for this initial error is compared with that of the growing mode. The solid line displays the growth of kinetic energy during the forecast time when the initial error is in the pattern as shown in Fig. 4a. In case the initial

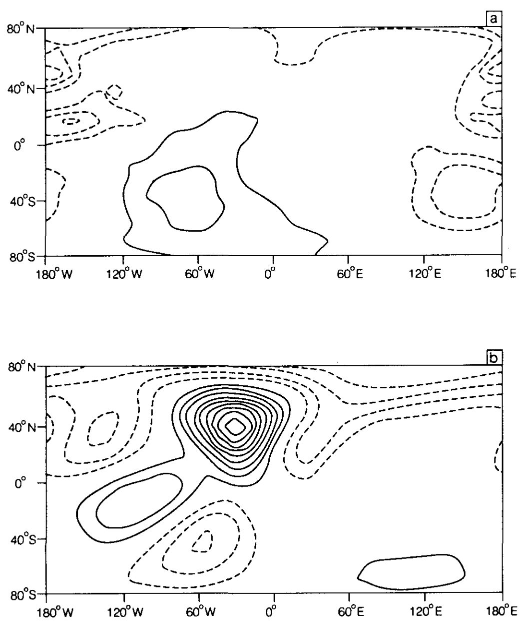

Fig. 3. Same as Fig. 1, but now for $t = 48$ h at grid point (35° W, 40° N).

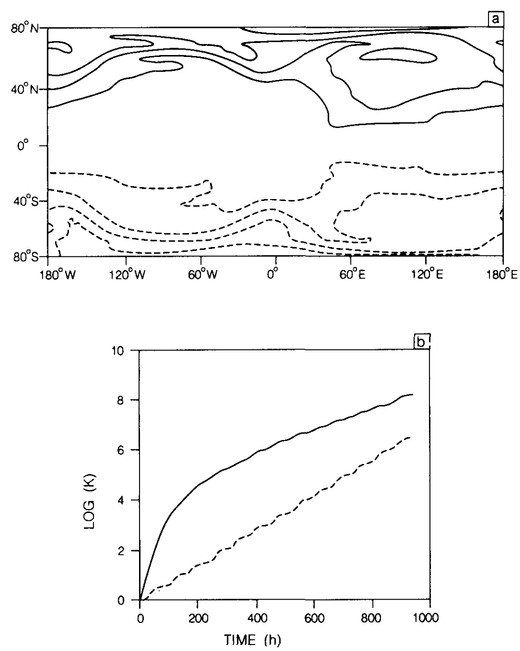

Fig. 4. (a) Initial error for $t = 600$ h at grid point (65° E, 40° N), contour interval is $3 \cdot 10^{-4}$ and (b) growth of the kinetic energy K for the unique growing mode of ψ (dashed line) and for the mode given in Fig. 4a (solid line).

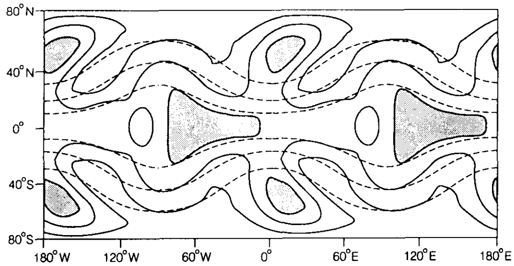

Fig. 5. Sensitivity plot of the stationary wave ψ for a forecast time of 48 h. Shaded areas indicate low sensitivity to error growth, contour interval is $5 \cdot 10^{-4}$. The stream function pattern is given by dashed lines.

error kinetic is completely in the growing mode the dashed line results. Clearly the initial error as depicted in Fig. 4a is not solely in the growing mode. The full line shows very rapid initial growth in the first few days due to dispersion reversal, followed by a period with growth which is slightly less than the exponential increase of kinetic energy of the unstable mode. For $t \to \infty$, the growth rate of the two error fields becomes the same. The wiggling of the curves in Fig. 4b results from the difference in kinetic energy of the real and imaginary phase of the error fields. We conclude that on time scales for which the assumption of linear growth is valid, error growth is not necessarily dominated by the exponential error growth.

We systematically studied the dependence of the maximal forecast error in p with respect to its geographical location. Fig. 5 displays the maximal forecast error in the streamfunction at p for every position of p on the globe. The forecast time is 48 h. For every position of p the initial error kinetic energy was the same. The figure shows minimum error growth in p when it is located in the troughs

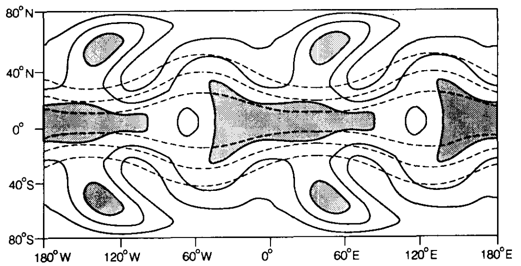

Fig. 6. The same as Fig. 5 but now for a traveling wave. Dashed lines shows the stream function pattern at $t = 48$ h.

and ridges of the stationary (2, 3)-wave, especially in the areas of weak winds close to the centers of high and low pressure. Error growth in p is large when it is located in middle latitudes and between the trough and ridge axes. It is especially large when p is located downstream of the troughs of the (2, 3)-wave.

So far we have only studied error growth for a stationary solution of the barotropic vorticity equation. We have extended this to a periodic solution by adjusting the strength of the solid body rotation. For $c = 0.26$ the solution has a period of 240 h. So, in 48 h, the wave travels a distance of 36° of longitude. For this solution we have again computed the maximal forecast error in p after 48 h as a function of the position of p. The resulting pattern as displayed by Fig. 6 is basically the same as the pattern of Fig. 5, except for a longitudinal phase shift of 36°. The positions of maximal and minimal error growth simply propagate with the basic (2, 3)-wave. The growth of error kinetic energy is the same for the stationary and the propagating solution. It only depends on the position of p with respect to the phase of the wave at the end of the forecast period.

Finally, as an example of a more realistic stream pattern we consider the case of a blocking over Western-Europe. For that, we took the analysis for 23 November 1988 00GMT and integrated this field for 48 h with the barotropic model, see Fig. 7. Observe that the blocking ridge is almost stationary. The ridge which initially was situated

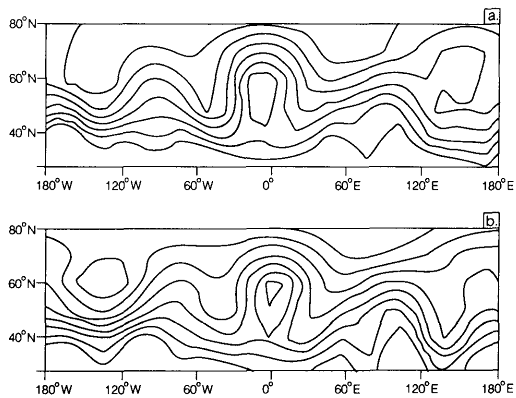

Fig. 7. (a) Analysis of the stream function pattern for 23 November 1988 00GMT at 500 mb and (b) after integrating for 48 h with the barotropic model. In both cases only part of the Northern Hemisphere is shown. Contour interval is $9 \cdot 10^6$ m^2/s.

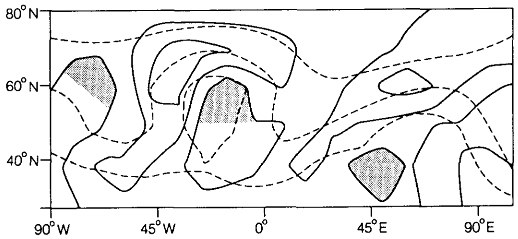

Fig. 8. Sensitivity plot for part of the pattern of Fig. 7a with a forecast time of 48 h. Shaded areas indicate low sensitivity to error growth, contour interval is $4 \cdot 10^{-4}$. The stream function pattern at $t = 48$ h is given by dashed lines.

at (95° W, 60° N) progressed during 48 h 15° eastward in the barotropic model. The sensitivity diagram as displayed in Fig. 8 seems to be related to the steam pattern in an easy manner. Areas of low or high gradients of the pressure fields yield a low or high sensitivity to error growth. This is an agreement with what we found in the previous examples.

6. Concluding remarks

This paper suggests a method for studying local error growth. We were able to determine initial error fields of a fixed kinetic energy which, for a given forecast time, maximize the error over a pre-chosen area. This maximum error yields a kind of upper limit to the error growth for this area and forecast time. In this way it may help to obtain better insight in the local and temporal predictability of the atmospheric circulation. Although we considered the error of the streamfunction field, the method can be used as well for example in studying local error growth on the vorticity field. Experiments performed with a barotropic model showed that dispersion reversal could result in a more rapid error growth than was to be expected from exponential mode growth. By dispersion reversal we mean that several modes cooperate in such a way that during the forecast time, maximum error is focussed onto the pre-chosen area. Initial errors as shown in Fig. 2a further inform about the areas which contribute to the final error. A subject for further study is the impact of realistic probability distributions of initial error fields.

In a forthcoming paper we shall consider to what extent local error growth, as studied here, can inform about skill prediction for an area.

7. Acknowledgments

I would like to thank J. D. Opsteegh, H. Tennekes and P. L. Houtekamer for their carefully reading of the manuscript and for giving valuable comments. Also thanks are due to W. T. M. Verkley for allowing us to use his barotropic model and to Mrs. S. J. M. Krooshof for preparing the plots. Further, I am very grateful to the reviewers for their remarks which resulted in an improvement in the presentation of the results.

8. Appendix

The adjoint equation clearly depends on the inner product defined for $\mathscr{F}$. Yet there is an easy correspondence between the resolvent of the adjoint equation for different inner products.

Let $\langle\, ,\, \rangle$ and $(\, ,\,)$ be two inner products on $\mathscr{F}$. Then there exists, (e.g., Packel, 1974), a linear operator $M: \mathscr{F} \mapsto \mathscr{F}$ such that

(a) $(x, y) = \langle x, My \rangle$ for all $x, y \in \mathscr{F}$,

(b) M^{-1} is defined.

Given a linear operator $T: \mathscr{F} \mapsto \mathscr{F}$, we denote the adjoint of T by T^* or T^0 depending on whether $\langle\, ,\, \rangle$ or $(\, ,\,)$ is used. We have

$$(x, T^0 y) = (Tx, y) = \langle Tx, My \rangle$$
$$= \langle x, T^* My \rangle = (x, M^{-1} T^* My)$$

for all $x, y \in \mathscr{F}$.

Therefore, T^0 is given by $T^0 = M^{-1} T^* M$.

As an example we apply the above to the kinetic energy inner product $\langle\, ,\, \rangle$ and the inner product $(\, ,\,)$ defined by

$$(f, g) = \iint_{S^2} fg \, \mathrm{d}s,$$

It is easy to see that $(f, g) = \langle f, -\Delta^{-1} g \rangle$. With L as defined in eq. (10) we can write

$$(L\varepsilon(t), \varepsilon(t)) = (R^0 L R \varepsilon(0), \varepsilon(0)) = (\varepsilon(t)_{|p})^2.$$

In this case we maximize the final error $\varepsilon(t)$ in p but now with constraint $(\varepsilon(0), \varepsilon(0)) = 1$. As before we have to look for the eigenvector of $R^0 L R$ with largest eigenvalue. Consequently the initial error $\varepsilon(0)$ is proportional to $R^0 \delta = \Delta R^* \Delta^{-1} \delta$.

REFERENCES

Courant, R. and Hilbert, D. 1953. *Methods of mathematical physics.* Vol. 1, New York: Interscience Publ.

Farrell, B. F. 1987. Optimal excitation of neutral Rossby waves. *J. Atmos. Sci. 45*, 163–172.

Farrell, B. F. 1990. Small error dynamics and the predictability of atmospherics flows. *J. Atmos. Sci. 47*, 2409–2416.

Lacarra, J. and Talagrand, O. 1988. Short-range evolution of small parturbations in a barotropic model. *Tellus 40A*, 81–95.

Le Dimet, F.-X. and Talagrand, O. 1986. Variational algorithms for analysis and assimilation of meteorological observations: theoretical aspects. *Tellus 38A*, 97–110.

Hall, M. C. G. and Cacuci, D. G. 1983. Physical interpretation of the adjoint functions for sensitivity analysis of atmospheric models. *J. Atmos. Sci. 40*, 2537–2546.

Lorenz, E. N. 1963. Deterministic nonperiodic flow. *J. Atmos. Sci. 20*, 130–141.

Machenhauer, B. 1979. The spectral method. *GARP Publ. series no. 17* II, 124–277.

Packel, E. W. 1974. *Functional analysis, a short course.* New York: Intext Inc.

Palmer, T. N. and Tibaldi, S. 1988. On the prediction of forecast skill. *Mon. Wea. Rev. 116*, 2453–2480.

Talagrand, O. and Courtier, P. 1987. Variational assimilation of meteorological observations with the adjoint vorticity equation. I: Theory. *Q. J. R. Meteorol. Soc. 113*, 1311–1328.

Thiébaux, H. J. and Morone, L. L. 1990. Short-term systematic errors in global forecasts: their estimation and removal. *Tellus 42A*, 209–229..

Zhang, Z. 1988. *The linear study of zonally asymmetric barotropic flows.* Ph.D. thesis, University of Reading, UK.